Cellulose (2005) 12:595–606
DOI 10.1007/s10570-005-9008-1

Direct observation of cellulose dissolution in subcritical and supercritical water over a wide range of water densities (550–1000 kg/m^3)

Yuko Ogihara[1], Richard L. Smith Jr.[1,*], Hiroshi Inomata[1] and Kunio Arai[1]
[1]*Research Center of Supercritical Fluid Technology, Tohoku University, Aoba-ku, Aramaki Aza Aoba-6-6-11, Sendai, 980-8579, Japan; *Author for correspondence (e-mail: smith@scf.che.tohoku.ac.jp; phone: +81-22-795-5863; fax: +81-22-795-5863)*

Received 10 April 2005; accepted in revised form 3 August 2005

Key words: Biomass, Cellulose, Microreactor, Supercritical water, Visualization

Abstract

Direct observations of the heating of microcrystalline cellulose (230 DP) in water at temperatures up to 410 °C and at pressures up to 700 MPa were made with a batch-type microreactor. Cellulose particles were found to dissolve with water over temperatures ranging from 315 to 355 °C at high pressures. Dissolution temperatures depended on water density and decreased from about 350 °C at a water density of 560 kg/m^3 to a minimum of around 320 °C at a water density of 850 kg/m^3. At densities greater than 850 kg/m^3, the dissolution temperatures increased and reached a value of about 347 °C at 980 kg/m^3. The cellulose dissolution temperatures were independent of heating rates for values ranging from 10 to 17 °C/s. The low dependence of dissolution temperatures on the heating rates is strong evidence for simultaneous dissolution and reaction of the cellulose. Different phenomena occurred depending on water density. At low densities, particles turned transparent and seemed to dissolve into the aqueous phase from the surface. From 670 to 850 kg/m^3, the cellulose particles visibly swelled just before completely collapsing and dissolving into the aqueous phase. The swelling probably increased water accessibility and particle surface area and thus lead to the lower dissolution temperatures observed. From 850 to 1000 kg/m^3, the particles required longer times to dissolve and many fine brown-like particles were generated as the particles dissolved. FT-IR spectra of the residues were analyzed. Residues formed from heating cellulose at high densities still retained some cellulose character whereas those as low densities had little cellulose character, especially in the O–H stretching vibration region.

Introduction

Direct observation of phenomena coupled with various forms of microscopy has lead to some remarkable findings in chemical and related fields. Aarts et al. (2004) studied the fluid–fluid interface in a phase-separated colloid-polymer dispersion and observed thermally induced capillary waves at the interface in real time giving insight into the process of liquid film formation and droplet coalescence. Scott et al. (2004) found that methane could be generated from FeO, $CaCO_3$-calcite and water at high temperatures and high pressures, thus demonstrating the existence of abiogenic pathways for hydrocarbon formation. Shen and Keppler (1997) determined by direct observation that the albite-H_2O system could be completely miscible at high temperatures and pressures thus showing the possibility of a hydrous mobile phase in the Earth's crust. Microscopy has been used not

only to elucidate significant new phenomena but also fundamental properties such as solubilities (Wang et al. 2004), viscosities (Audetat and Keppler 2004) or occurrences such as the roughening transition of ice Ih (Maruyama 2005).

Carbohydrates have also been studied with microscopy techniques. Mazzobre et al. (2003) used microscopy and calorimetry to evaluate sugar crystallization kinetics. Michael et al. (2000) studied the interaction of cellulose with amine oxide solvents and found that fibers tended to swell longitudinally during dissolution and this along with ^{13}C CPMAS NMR data allowed those authors to conclude that initial penetration of the solvent occurred between molecular cellulose sheets.

The conformation and packing arrangements of crystalline cellulose allomorphs (type Ib, II, III_1, IV_1, IV_2) have been reviewed by Zugenmaier (2001) and previously by O'Sullivan (1997). As noted in those reviews, all celluloses show a ribbon-like shape with the ribbons being arranged almost flat in intrasheets that held together tightly to form the crystalline structure of the material. For the case of cellulose I, allomorphs are packed in a parallel chain arrangement, whereas regenerated or mercerized cellulose or so-called cellulose II, the allomorphs are arranged antiparallel. The conversion from cellulose I to cellulose II can be accomplished by intracrystalline swelling in NaOH and washing and drying that presumably allows the allomorphs to achieve antiparallel arrangement. Besides aqueous NaOH solutions, treatment with other solvents such as hydrazine, ethylenediamine solutions or high-temperature water (Sasaki et al. 2003a) has also been noted to promote allomorph rearrangement. Of these, high-temperature water is the solvent of interest in this work.

The critical point of water occurs at a temperature of 373.946 °C and at a pressure of 22.064 MPa, in which water's density is 322 kg/m^3 (Fernández-Prini and Dooley 1997). Below this temperature and at densities greater than 322 kg/m^3, water is generally called subcritical water. At temperatures above 100 °C, liquid water is referred to as being at hydrothermal conditions or as high-temperature water. Above the temperature and pressure of the critical point, water is generally called supercritical water (SCW). As water is brought to its supercritical state, its properties and reactivity change greatly and these features have generated much interest for many practical processes (Arai and Adschiri 1999). For example, researchers are considering water as the solvent for processes to liquefy or process biomass (Antal et al. 2000; Zhong et al. 2002; Qu et al. 2003; Sasaki et al. 2003b; Feng et al. 2004a, b; Goto et al. 2004). Cellulose, the main part of woody biomass, has been shown to decompose to oligosaccharides and glucose under hydrothermal conditions and in SCW by many research groups (Modell 1977; Bobleter 1994; Luijkx et al. 1995; Saka and Ueno 1999; Sasaki et al. 2000; Laser et al. 2002).

Sasaki et al. (2000) used microscopy and found that microcrystalline cellulose dissolves in high density (1000 kg/m^3) water at high temperatures (350 °C) thus offering a possible explanation for the high reaction rates measured for SCW that were reported in an early work by Adschiri et al. (1993). Although it is known that the reaction pathways of cellulose depend on heating rate, heating time, and water density, little research has been done to examine the phenomena occurring as cellulose is heated in water and undergoes hydrolysis. The phase behavior of cellulose under reactive conditions or so-called reactive phase behavior is of interest not only for scientific reasons related to understanding chemical transformations but also for technological development regarding the use of biomass as a sustainable resource.

In this work, we use microscopy to study the behavior of microcrystalline cellulose in water as it is heated from ambient conditions to those of high-temperature (ca. 400 °C) and high-pressure (ca. 50–700 MPa) with the objective to determine the nature of the phase transformations that occur. We use a batch microreactor that is loaded with water and cellulose and then its contents are rapidly heated. The complete contents of the cell are visible at all times and at all conditions. We vary the water loaded into the cell to have densities in the range of 500–1000 kg/m^3 and use heating rates up to 17 °C/s. Product residues are analyzed with infrared spectroscopy.

Materials and methods

Microcrystalline cellulose used in the experiments was obtained from Merck (Tokyo) and had a stated viscosity average degree of polymerization (DP_V) of 230 and a relative crystallinity of 77.8%.

Water used in the experiments was double-distilled and had a resistivity greater than 18 MΩ.

Reactions and visual observations of water and cellulose mixtures were performed with a microreactor that consisted of a Bassett-type (Bassett et al. 1993) hydrothermal diamond anvil cell (HDAC) with an arrangement that is described in some of our previous works (Fang et al. 2000). The apparatus is shown in Figure 1. Type I brilliant-cut diamonds (3.3–3.5 mm girdles, 1 mm culets) were used for the anvils of the apparatus to confine solutions contained within metal gaskets. The metal gaskets consisted of thin sheets of 304 stainless steel (0.25 mm thick) that were drilled to have 0.5 mm holes, which formed the experimental chambers. After pre-indention, the chamber volumes in the gaskets were approximately 40–50 nL. Loading of the chambers with solutions is described below. Rapid heating was performed with two homemade microheaters made from 0.7 mm Mo wire to each have approximately 1 Ω resistance. Heating rates up to 17 °C/s were used with total heating time being generally less than 50 s. The heaters served as supports for the diamond anvils. Temperature was measured on both the lower and upper anvil by K-type thermocouples with a data logger (Agilent 34970A, Palo Alto) and computer at a frequency of 10 Hz. Images were viewed with a microscope (Olympus SZX ZB12, Tokyo) at up to 100× magnification and captured with a CCD camera (Olympus CS230, Tokyo). Infrared measurements were made of the residues with an FTIR microscope (JASCO Irtron IRT-30, Tokyo) with 32 scans, 5 s exposure, at 4 cm^{-1} resolution.

Experiments are performed in the HDAC occur under batch conditions, which means that specification of temperature and density determine pressure for a pure-component, single-phase system. In this work, the systems studied were dilute mixtures and so we used the following procedure for loading and for estimating pressures. First, the gasket was fixed to the lower anvil with a small amount of cement placed around the gasket periphery and pre-indented. A small amount of microcrystalline cellulose was loaded into the gasket chamber by using a fine 0.1 mm diameter wire along with static electricity. Then, a small amount of water was placed on the upper anvil, which was held there due to surface tension until the two anvils were joined. Density of the loaded water was changed by varying the amount of argon gas trapped into the gasket chamber during joining of the anvils. In general, argon gas was

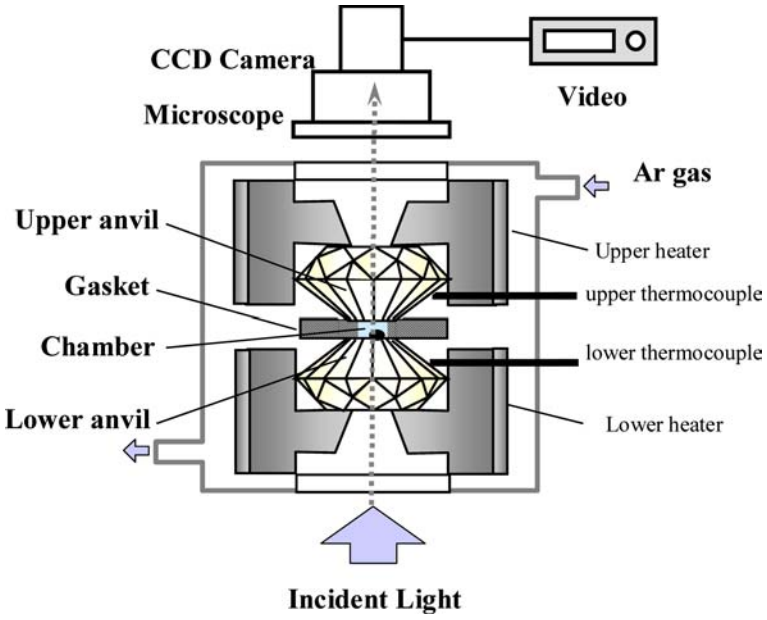

Figure 1. Experimental apparatus.

flowed around the experimental chamber when loading.

After pressing the two anvils together and applying pressure, the solution would appear as either a clear (aqueous) liquid phase that contained cellulose particles or as a mixture of water and cellulose particles that contained a gas bubble. The density of the solution was determined by noting the temperature of the gas bubble disappearance during heating. The temperature at which the included gas bubble became single phase with the aqueous phase is denoted as the homogeneous temperature (T_h).

Since heating of the chamber is an isochoric process, knowledge of the gas bubble disappearance, T_h, allows one to know the system density, ρ, as a point on the saturation boundary and thus allows one to estimate the pressure in the chamber according to methods in the literature (Bassett et al. 1993) and those described in our previous research (Fang et al. 1999, 2004). The calculated pressure at which the loaded gas bubble becomes homogeneous with the aqueous phase is denoted as the homogeneous pressure, P_h. The temperature and pressure at which the cellulose particles seem to dissolve are denoted as the dissolution temperature, T_d, and dissolution pressure, P_d, respectively. The P_d was calculated from the system density and the dissolution temperature.

In this work, we used the equation of state of Wagner and Pruss (2002) for the properties of water. The pressures in the chamber were calculated from the temperature and density of the system. Knowledge of pressure in the chamber is of technological interest since temperature and pressure can be conveniently controlled under flow conditions.

Results and discussion

Conditions of each experimental run are shown in Table 1, which gives experimental heating rates, observed disappearance temperatures, T_h, calculated P_h, system densities, and cellulose particle dissolution conditions. Cellulose particles were noted to completely dissolve into the aqueous phase at disappearance temperatures, T_d. The maximum nominal pressure, P_{max}, attained at a nominal temperature of 410 °C is shown in Table 1 for reference.

Direct observations

At all density conditions and high heating rates (10–17 °C/s), cellulose particles were found to become homogeneous with water without any added catalyst or additives at temperatures in the range from 315 to 355 °C at high pressures (37–560 MPa). For cellulose particles that were heated at low heating rates (2 °C/s), brown solids appeared without cellulose crystal disappearance. Phenomena such as convective mixing, crystalline particles turning transparent, crystal edges melting, and particle dissolution were observed as shown by a series of snapshots (Figures 2–4) for the given densities and heating profiles.

At a water density of 660 kg/m^3, intense convection occurred in the reactor during heating causing violent mixing among cellulose and water solvent (Figure 2, Run 5). The convective mixing at this density (660 kg/m^3) ceased when the aqueous phase reached the homogeneous temperature, T_h at 322 °C. Cellulose particles underwent dissolution without changing shape and became transparent with a skeletal framework and then, without any apparent movement, the particles became completely homogeneous with water at a T_d of 350 °C (37 MPa). Cooling of the DAC and examination of the anvils revealed a small amount of clear residue, that is discussed in the analysis section.

At a water density of 790 kg/m^3 (Figure 3, Run 10), no convective mixing was observed during heating and T_h occurred at 255 °C. The cellulose particles underwent dissolution at a T_d of 328 °C (100 MPa) and a few solid particles were generated just after cellulose particle dissolution. The T_d was considerably lower than that of the previous case. After cooling, a larger amount of residue than that of the previous case was apparent on the anvils.

At a water density of 980 kg/m^3 (Figure 4, Run 18), no convective mixing was observed during heating and T_h occurred at 61 °C (not shown). At 330 °C, cellulose particle dissolution seemed to begin with the particles becoming transparent. The cellulose particles underwent complete dissolution at a T_d of 344 °C (560 MPa). For this case, the particles seemed to require longer times for dissolution and dissolved along the surface boundaries. Many fine brown-like particles were generated at the high-temperature, high-pressure

Table 1. Experimental runs with heating rates, homogeneous temperatures, T_h, and pressures, P_h, crystal disappearance temperatures, T_d, and pressures, P_d, and maximum pressures calculated at the system density and nominal maximum temperature, 410 °C.

Run No.	Heating rate [°C/s]	T_h [°C]	P_h [MPa]	ρ [kg/m^3]	T_d [°C]	P_d [MPa]	P_{max} [MPa]
1	16.6	356	17.9	548	346	12	50
2	12.7	353	17.1	562	350	15	53
3	16.3	333	13.4	633	348	25	76
4	14.6	330	12.9	641	350	29	80
5	14.1	323	11.7	660	351	36	89
6	10.0	322	11.6	661	352	38	90
7	17.3	319	11.1	670	337	27	95
8	12.7	276	6.0	757	324	64	168
9	14.9	258	4.5	787	328	97	206
10	13.8	255	4.3	791	328	102	211
11	12.8	216	2.1	846	323	168	303
12	14.3	205	1.7	859	317	181	329
13	14.9	174	0.9	893	326	262	408
14	12.6	137	0.3	929	328	351	507
15	14.2	103	0.1	956	341	456	594
16	15.7	91.5	0.1	964	342	483	622
17	12.9	81.9	0.1	970	345	510	644
18	13.7	60.9	0.0	983	346	555	692

conditions. After cooling, a large amount of residue was apparent as shown in Figure 4.

Analysis

Representative infrared spectra of residues obtained at the densities described in the previous section are shown in Figure 5. Spectra for microcrystalline cellulose, cellobiose, and glucose are shown for reference. Typical spectral features of cellulose are the broad bands due to O–H stretching vibration in the 3200–3400 cm^{-1} region, the C–H stretch at 2900 cm^{-1}, and the deformation vibrations of the HC_6H and COH groups in the 1400–1500 cm^{-1} region (Zhbankov et al. 2002). Spectra for the lowest densities were difficult to obtain because the sample residue so small.

For both residues at the lower densities (660 and 790 kg/m^3), the IR spectra exhibited a complete absence of cellulose character as shown by the lack of O–H stretching vibration from 3200 to 3400 cm^{-1} and characteristic C–H stretching vibration at 2900 cm^{-1}. Further, the samples

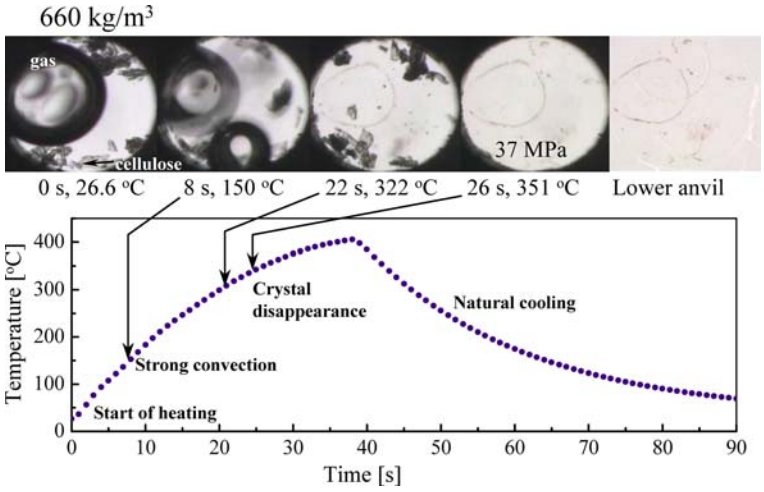

Figure 2. Cellulose reactive phase behavior and heating profile at 660 kg/m^3. See Table 1, Run 5 for detailed conditions.

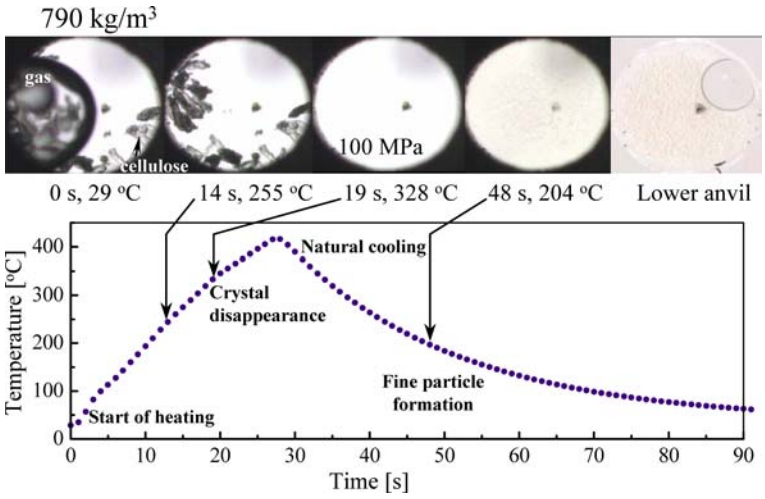

Figure 3. Cellulose reactive phase behavior and heating profile at 790 kg/m^3. See Table 1, Run 10 for detailed conditions.

showed only very weak peaks in the ranges of C–H bending vibration (1440 cm^{-1}). It is known that reaction of cellulose in water at high heating rates produces glucose that reacts further via tautomerism, retro-Aldol condensation, and dehydration to form aldehydes and furfurals (Sasaki et al. 1998, 2002). For runs at the lower densities (Runs 1–10), the cell contents were transparent (clear) when cooled. Since only trace amounts of residues remained on the anvils in many cases, it is expected that any trace amounts of products present, such as aldehydes or furfurals, probably volatilized when the cell was opened.

At the higher density (980 kg/m^3, Run 18), both O–H stretching vibration and C–H stretching vibration became apparent (Figure 5). The cellulose-like character of the residue under these conditions is evidence that the reaction proceeded either more slowly at high water densities or that the reaction proceeded through different pathways to produce polymerization products. Heating of cellulose at high water density conditions promotes the formation of 'glucose char' (Fang et al. 2004). The presence of the C=0 stretching vibration at 1700 cm^{-1} can probably be attributed to the presence of compounds such as pyruvaldehyde or glyceraldehyde that tend to be present in 'glucose char' or glucose polymerization products. The formation of polymerization products from hydrothermal reactions has been reported by Sakaki et al. (2002), who noted that precipitates contained polymerized saccharides from hexamer to eicosamer or higher. From Figure 5, polymerized saccharides could be another possibility for the products formed under these extreme conditions of temperature (410 °C) and pressure (692 MPa).

Some observations can be made by comparing the spectra of the residues formed at water densities of 660, 790, and 980 kg/m^3 (Figure 5). First, the spectra are clearly dissimilar indicating that different products were formed at the given densities. It is important to note that the reaction times and heating rates for these runs were roughly about the same (Table 1). Second, there seems to be a trend from more cellulose character (high density) to less cellulose character (low density). Considering the previous observations on dissolution temperatures, this most likely means that simultaneous dissolution and reaction occur, with reaction probably being faster at the lower densities. This would be consistent with reports in the literature (Adschiri et al. 1993; Sasaki et al. 2004) that note an increase in the reaction rate constant for hydrolysis of cellulose, as conditions move from those of subcritical (high density) to supercritical (low density).

Variation of dissolution temperatures with density

A number of experiments were performed at densities ranging from 550 to 1000 kg/m^3 to examine the variation in the dissolution temperature of the

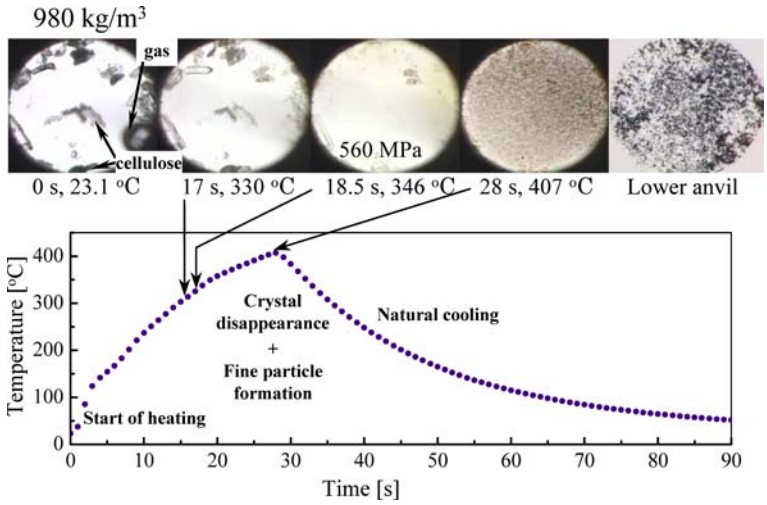

Figure 4. Cellulose reactive phase behavior and heating profile at 980 kg/m^3. See Table 1, Run 18 for detailed conditions.

cellulose particles with temperature. Results are shown in Figure 6, which plots the observed dissolution temperatures vs. water density in the microreactor. As shown in Figure 6, dissolution temperature varied smoothly with density and exhibited a minimum at water densities in the range of 800 kg/m^3. We examined this trend in more detail by comparing 0.1 s or 0.2 s interval photographs of the dissolution at in the low (550–660 kg/m^3), intermediate (700–860 kg/m^3) and high (900–1000 kg/m^3) density region as described in a section below.

Variation of heating rate

Whether the microcrystalline cellulose undergoes reaction or dissolution or some combination of these processes during the heating was a question that is of fundamental interest. To attempt to answer this question, we made a number of runs where the heating rates were varied for the given range of densities. As shown in Figure 6, cellulose particles tended to dissolve at approximately the same temperatures independent of the heating rates used (10–17 °C/s). This is strong evidence that both dissolution and reaction took place during the heating of the cellulose. The lower density conditions probably promoted breakage of intermolecular hydrogen bonds more so than intramolecular hydrogen bonds. Sasaki et al. (2004) have noted that cellulose microfibrils become swollen and then are cleaved and these products form crystallites in SCW at 400 °C and 25 MPa, whereas at subcritical conditions of 320 °C and 25 MPa, cellulose microfibrils are cleaved and then swell or dissolve before forming crystallites. In their experiments for the supercritical case, the DP of the microfibril did not change significantly with conversion at short reaction times. Although we have no method to measure DP of such small amounts of material, the lack of sensitivity of the dissolution temperatures with heating rates is strong evidence that breaking of intermolecular hydrogen bonds occurs, which allows the microfibrils to dissolve in SCW. The

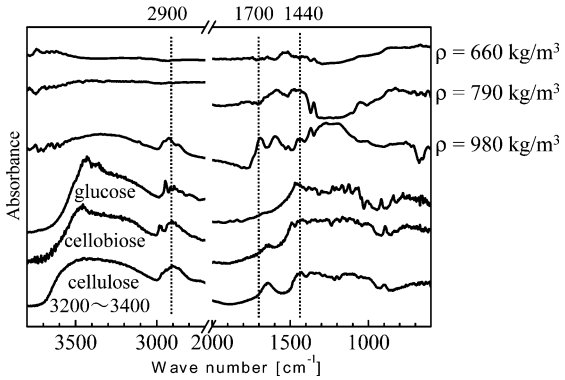

Figure 5. Infrared spectra of residues at 660, 790, and 980 kg/m^3. See Table 1, Runs 5, 10, and 18, for detailed conditions.

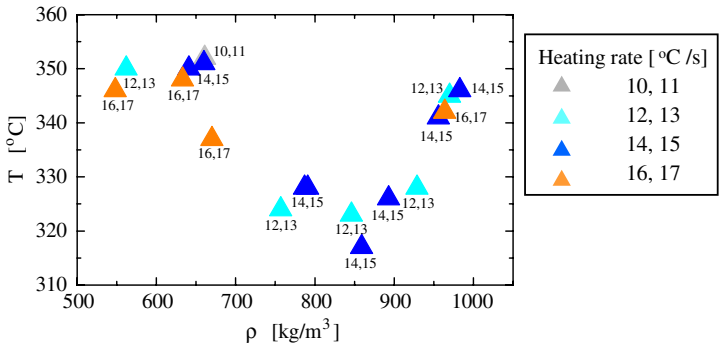

Figure 6. Temperature of cellulose dissolution over a range of densities (550–980 kg/m^3) and heating rates (10–17 °C/s). Heating time is on the order of 30 s.

results presented in this work show a clear density dependence on the dissolution temperatures of cellulose when heated in water.

Dissolution processes

Short time interval (0.1 s or 0.2 s) photographs of the dissolution processes for three densities (660, 790, and 980 kg/m^3) are shown in Figure 7. At 660 kg/m^3 (Figure 7a), cellulose particles became transparent and seemed to dissolve over a 5 °C temperature span (344–348 °C) without any discernable motion. At 790 kg/m^3 (Figure 7b), cellulose particles seemed to dissolve over a 10–12 °C temperature span (318–328 °C). Just prior to the dissolution process, there was considerable particle expansion that can be seen in the marked areas (dashed circles) of Figure 7b over the temperature range of 312–320 °C. At 980 kg/m^3, the cellulose particles seemed to take much longer to dissolve into the aqueous phase (Figure 7c). In fact, dissolution of the cellulose particles occurred over a temperature range of ca. 16 °C (344–348 °C) for the high density runs. These different phenomena are discussed next in view of the cellulose microstructure.

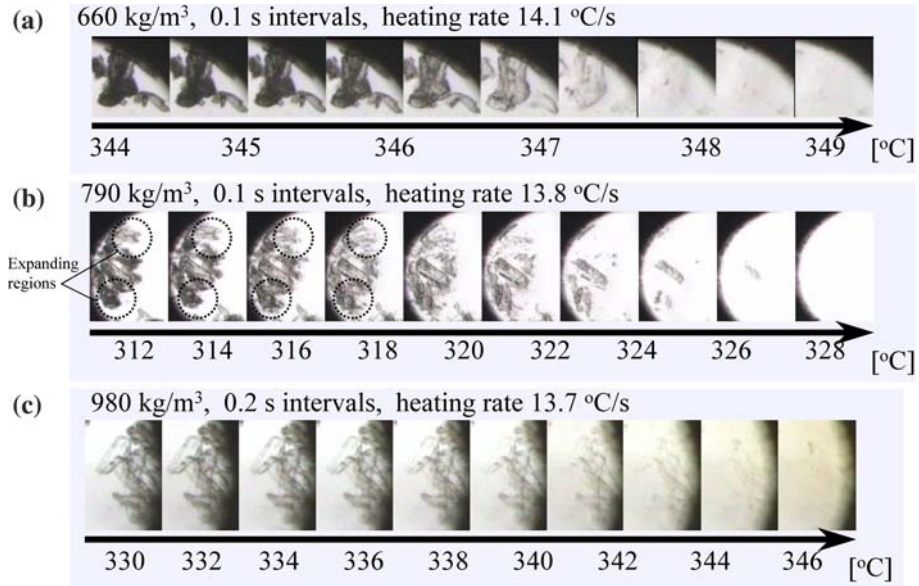

Figure 7. Short time interval micrographs for cellulose decomposition at 660, 790, and 980 kg/m^3 See Table 1, runs 5, 10, and 18, for detailed conditions.

Discussion on dissolution processes

Microcrystalline cellulose has a high degree of crystallinity but also contains amorphous regions. In the low density region, particles tended to become clear and seemed to undergo surface melting that is caused by surface hydrolysis. The comparatively narrow temperature range of particle dissolution for the low water density (500–660 kg/m^3) seemed to be evidence that the water had very high activity with accessible areas of the cellulose at the maximum pressure (37 MPa). On the other hand, in the intermediate density region (700–860 kg/m^3), the higher pressures (100 MPa) probably caused more of the water to penetrate amorphous regions, which, caused particle swelling to occur when heated. The swelling was reproducible over a range of densities and was probably responsible for the gradual lowering of the dissolution temperatures. It can be inferred that gradual splitting of the cellulose allomorph chains occurred during heating that would mean breakage of intermolecular hydrogen bonds. The increased water accessibility provided by intermolecular hydrogen bond breakage most likely promoted surface hydrolysis compared with high density cases.

At very high water densities (980–1000 kg/m^3) corresponding to pressures as high as 700 MPa at the given temperature, the increased hydrostatic pressure of the water may have caused changes in the cellulose crystallinity, but almost certainly lowered the water mobility within both crystalline and amorphous regions of the cellulose. Some apparent changes in polymer crystallinity have been noted in the literature, for polymers such as nylon 6/6 at very high pressures (Smith et al. 1999). For that case, nylon 6/6 was observed to have crystalline-like features after heating for 12 min at 272 °C in the presence of water at high pressure (848 MPa) even though nylon 6/6 has a melting point of around 255 °C at atmospheric pressure. For the case of microcrystalline cellulose, there may be a similar effect on the material and extremely high pressures probably induce some crystallinity and make some regions of the cellulose structure less accessible to water or make bound water much less active than free water.

At lower densities, microcrystalline cellulose possibly undergoes internal hydrolysis but mainly undergoes surface reaction. The higher diffusion coefficient of water compared with the higher density conditions probably leads to narrow dissolution ranges for the low density cases. As water density increases, water penetrates more into the amorphous regions and between cellulose microfibrils. As the material is heated, an expansion probably causes fragmentation that increases the cellulose surface area, which is probably responsible for the gradual decrease in the dissolution temperatures with increasing water density. As water density is increased beyond a certain point, compression probably begins to restrict fragmentation and may lead to an increase in crystallinity of the cellulose. Although this is difficult to confirm, the increased pressures (700 MPa) would greatly restrict water transport into and out of any structure, which would lead to an increase in dissolution temperature due to lower reactivity.

The competing effects between water penetration and intra-microfibril expansion and compression most likely cause the cellulose dissolution temperatures to gradually decrease and then sharply increase with increasing water density. In other words, at lower water densities, effects of high water penetration associated with high water diffusivities and microfibril expansion would cause a decrease in cellulose crystal dissolution temperatures whereas at higher water densities associated with low water diffusivities, effects of low water penetration associated with low water diffusivities and microfibril compression would cause an increase in dissolution temperatures.

There is further evidence for this in the literature both from experimental and theoretical results. Saka and Ueno (1999) reported that the pattern of cellulose hydrolysis of various celluloses (Avicel, Lyocell) to glucose in SCW generally were not influenced by the differences in crystallographic nature of the celluloses, but rather by the amorphous regions and bound water, which seemed to play a greater role than the degree of crystallinity. In that work and later work, Ehara and Saka (2002) proposed that free water possibly acts as SCW as conditions of temperature and pressure changed within the hydrothermal or supercritical system, and this would lead to both internal and surface hydrolysis of the cellulose microfibrils. This seems to occur in our experiments, which show apparent expansion of some particles during the heating process. However, in this work, we show a clear

quantitative trend of dissolution temperatures with water density.

In simulations, Ito et al. (2002) studied small (54 glucose units) arrangements of monoclinic crystalline cellulose of Iβ phase in subcritical and SCW at densities of 310, 880, and 1000 kg/m^3. Those authors found that the population of hydrogen bonds between cellulose chains decreases to half as the temperature increases from room temperature to about 475 °C. Lowering the number of hydrogen bonds in the crystalline structure would make it more likely to split off and undergo surface hydrolysis. Experimental evidence exists for this from Sasaki et al. (2004) as discussed below. Further, Ito et al. (2002) found that the population of hydrogen bonds between cellulose chains decreases with increasing water density. This would support our observation that increasing water density above a certain density value causes the dissolution temperatures to increase. Interestingly, those authors show a minimum in breakup period for cellulose chains as a function of density that would somewhat correspond to results in our Figure 5 for dissolution temperature vs. density.

Sasaki et al. (2004) showed that the relative crystallinity of the residues from conversion of microcrystalline cellulose in water did not vary appreciably over a range of temperatures (290–380 °C) at 25 MPa. They concluded from the lack of variation in the residue crystallinity showed that the cellulose conversion occurs heterogeneously and the cellulose maintains its crystalline structure on reaction from 290 to 380 °C at 25 MPa. At these conditions, the density of the aqueous phase varies from about 450 kg/m^3 (380 °C, 25 MPa) to 760 kg/m^3 (290 °C, 25 MPa), which is within the range of our experiments. Although our heating times under batch conditions (ca. 15 s) were somewhat longer than the range of flow experiments (0.02–13.1 s) of Sasaki et al. (2004), it can be seen that microcrystalline cellulose studied in this work became homogeneous with water over a wide range of densities (Figures 2–4) at fairly narrow temperature ranges (Figure 6) and at temperatures much lower than the critical temperature of water (374 °C). The data in Figure 5 are strong evidence that swelling, hydrolysis and dissolution, occurred simultaneously.

Sasaki et al. (2003b) showed that the form of cellulose precipitates can be transformed from cellulose I to cellulose II by treatment with water at supercritical conditions. The present work shows that there is a density dependence to the transformation as shown by quantitative data of Table 1 and Figure 5.

Conclusions

Visual observation of the dissolution of microcrystalline cellulose in water during heating shows that cellulose particle dissolution depends on water density. The dissolution temperatures change systematically with density and show a minimum temperature of dissolution at densities around 800 kg/m^3. Cellulose particles noticeably swelled when heated at densities from 600 to 800 kg/m^3. The swelling probably increases the water accessibility to parts of the cellulose particle, which causes the temperature at which cellulose becomes homogeneous with water to decrease with density from 500 to 800 kg/m^3. At high water densities (>900 kg/m^3), the dissolution temperatures increased and approached those at the lower densities (500 kg/m^3). The high density conditions probably restricted water access to various regions of the cellulose and the increased pressure may have caused the cellulose to change in crystallinity or packing of the cellulose allomorphs. At the higher water densities, brown-like oils appeared but these could not be identified and will be a subject of future work. Further experiments are needed on other types of biomass, lignin, and cellulose including phase studies with solvents of different hydrogen bonding character.

Acknowledgement

The authors gratefully acknowledge the Ministry of Education, Science, Sports and Culture for partial financial support of this research.

References

Aarts D.G.A.L., Schmidt M. and Lekkerkerker H.N.W. 2004. Direct visual observation of thermal capillary waves. Science 7: 847–850.

Adschiri T., Hirose S., Malaluan R. and Arai K. 1993. Noncatalytic conversion of cellulose in supercritical and subcritical water. J. Chem. Eng. Jpn 26: 676–680.

Antal M.J., Allen S.G., Schulman D., Xu X.D., Divilio R.J., 2000. Biomass gasification in supercritical water, Ind. Eng. Chem. Res. 39: 4040–4053.

Arai K. and Adschiri T. 1999. Importance of phase equilibria for understanding supercritical fluid environments. Fluid Phase Equilib. 158–160: 673–684.

Audetat A. and Keppler H. 2004. Viscosity of fluids in subduction zones. Science 303: 513–516.

Bassett W.A., Shen A.H., Bucknum M. and Chou I.M. 1993. A new diamond-anvil cell for hydrothermal studies to 2.5 GPa and from −190 to 1200 °C. Rev. Sci. Instrum. 64: 2340–2345.

Bobleter O. 1994. Hydrothermal degradation of polymers derived from plants. Prog. Polymer. Sci. 19: 797–841.

Ehara K. and Saka S. 2002. A comparative study on chemical conversion of cellulose between the batch-type and flow-type systems in supercritical water. Cellulose 9: 301–311.

Fang Z., Minowa T., Smith R.L., Ogi T. and Kozinski J.A. 2004. Liquefaction and gasification of cellulose with Na_2CO_3 and Ni in subcritical water at 350 °C. Ind. Eng. Chem. Res. 43: 2454–2463.

Fang Z., Smith R.L. Jr., Inomata H. and Arai K. 1999. Phase behavior and reaction of polyethylene terephthalate-water systems at pressures up to 173 MPa and temperatures up to 490 °C. J. Supercr. Fluids 15: 229–243.

Fang Z., Smith R.L., Inomata H., Arai K. 2000. Phase behaviour and reaction of polyethylene in supercritical water at pressures up to 2.6 Gpa and temperatures up to 670 °C. J. Supercrit. Fluids 16: 207–216.

Feng W., van der Kooi H.J. and de Swaan Arons J. 2004a. Biomass conversions in subcritical and supercritical water: driving force, phase equilibria, and thermodynamic analysis. Chem. Eng. Proc. 43: 1459–1467.

Feng W., van der Kooi H.J. and de Swaan Arons J. 2004b. Phase equilibria for biomass conversion processes in subcritical and supercritical water. Chem. Eng. J. 98: 105–113.

Fernández-Prini R. and Dooley R.B. 1997. The International Association for the Properties of Water and Steam, Erlangen, Germany, September, Release on the IAPWS Industrial Formulation 1997 for the Thermodynamic Properties of Water and Steam. (http://www.iapws.org/).

Goto M., Obuchi R., Hirose T., Sakaki T. and Shibata M. 2004. Hydrothermal conversion of municipal organic waste into resources. Bioresour. Technol. 93: 279–284.

Ito T., Hirata Y., Sawa F. and Shirakawa N. 2002. Hydrogen bond and crystal deformation of cellulose in sub/supercritical water. Jpn. J. Appl. Phys. 41: 5809–5814.

Laser M., Schulman D., Allen S.G., Lichwa J., Antal M.J. Jr. and Lynd L.R. 2002. A comparison of liquid hot water and steam pretreatments of sugar cane bagasse for bioconversion to ethanol. Bioresour. Technol. 81: 33–44.

Luijkx G.C.A., van Rantwijk F., van Bekkum H. and Antal M.J. Jr 1995. The role of deoxyhexonic acids in the hydrothermal decarboxylation of carbohydrates. Carbohydr. Res. 272: 191–202.

Maruyama M. 2005. Roughening transition of prism faces of ice crystals grown from melt under pressure. J. Cryst. Growth 275: 598–605.

Mazzobre, M.F., Aguilera J.M. and Buera M.P. 2003. Microscopy and calorimetry as complementary techniques to analyze sugar crystallization from amorphous systems. Carbohydr. Res. 338: 541–548.

Michael M., Ibbett R.N., Howarth O.W. 2000. Interaction of cellulose with amine oxide solvents. Cellulose 7: 21–33.

Modell M. 1977. Reforming of glucose and wood at critical conditions of water. Mech. Eng. 99: 108–108.

OSullivan A.C. 1997. Cellulose: the structure slowly unravels. Cellulose 4: 173–207.

Saka S. and Ueno T. 1999. Chemical conversion of various celluloses to glucose and its derivatives in supercritical water. Cellulose 6: 177–191.

Sakaki T., Shibata M., Sumi T. and Yasuda S. 2002. Saccharification of cellulose using a hot-compressed water-flow reactor. Ind. Eng. Chem. Res. 41: 661–665.

Sasaki M., Kabyemela B., Malaluan R.M., Hirose S., Takeda N., Adschiri T. and Arai K. 1998. Cellulose hydrolysis in subcritical and supercritical water. J. Supercr. Fluids 13: 261–268.

Sasaki M., Fang Z., Fukushima Y., Adschiri T. and Arai K. 2000. Dissolution and hydrolysis of cellulose in subcritical and supercritical water. Ind. Eng. Chem. Res. 39: 2883–2890.

Sasaki M., Furukawa M., Minami K., Adschiri T. and Arai K. 2002. Kinetics and mechanism of cellobiose hydrolysis and retro-Aldol condensation in subcritical and supercritical water. Ind. Eng. Chem. Res. 41: 6642–6649.

Sasaki M., Adschiri T. and Arai K. 2003a. Production of cellulose II from native cellulose by near- and supercritical water solubilization. J. Agric. Food Chem. 51: 5376–5381.

Sasaki M., Adschiri T. and Arai K. 2003b. Fractionation of sugarcane bagasse by hydrothermal treatment. Bioresour. Technol. 86: 301–304.

Sasaki M., Adschiri T. and Arai K. 2004. Kinetics of cellulose conversion at 25 MPa in sub- and supercritical water. AIChE J. 50: 192–202.

Scott H.P., Hemley R.J., Mao H.K., Herschbach D.R., Fried L.E., Howard W.M., Bastea S. 2004. Generation of methane in the Earth's mantle: In situ high pressure-temperature measurements of carbonate reduction. Proc. Natl. Acad. Sci. 101: 14023–14026.

Shen A.H. and Keppler H. 1997. Direct observation of complete miscibility in the albite-H_2O system. Nature 385: 710–712.

Smith R.L. Jr., Fang Z., Inomata H. and Arai K. 1999. Phase behavior and reaction of nylon 6/6 in water at high temperatures and pressures. J. Appl. Polym. Sci. 76: 1062–1073.

Wagner W. and Pruss A. 2002. The IAPWS formulation 1995 for the thermodynamic properties of ordinary water substance for general and scientific use. J. Phys. Chem. Ref. Data 31: 387–535.

Wang H.M., Henderson G.S. and Brenan J.M. 2004. Measuring quartz solubility by in situ weight-loss determination using a hydrothermal diamond cell. Geochim. Cosmochim. Acta 68: 5197–5204.

Qu Y., Wei X. and Zhong C. 2003. Experimental study on the direct liquefaction of *Cunninghamia lanceolata* in water. Energy 28: 597–606.

Zhbankov R.G., Firsov S.P., Buslov D.K., Nikonenko N.A., Marchewka M.K. and Ratajczak H. 2002. Structural physico-chemistry of cellulose macromolecules. Vibrational

spectra and structure of cellulose. J. Mol. Struct. 614: 117–125.

Zhong C., Peters C.J. and de Swaan Arons J. 2002. Thermodynamic modeling of biomass conversion processes. Fluid Phase Equilib. 194–197: 805–815.

Zugenmaier P. 2001. Conformation and packing of various crystalline cellulose fibers Prog. Polym. Sci. 26: 1341–1417.